

## ATLAS Higgs Searches

---

Nansi Andari<sup>\* †</sup>

Laboratoire de l'Accélérateur Linéaire, IN2P3/CNRS, Université Paris-Sud 11, Orsay, France

E-mail: [andari@lal.in2p3.fr](mailto:andari@lal.in2p3.fr)

A combined search for the Standard Model Higgs boson with the ATLAS experiment at LHC using datasets corresponding to integrated luminosities from 1.0 to 2.3  $\text{fb}^{-1}$  of pp collisions at  $\sqrt{s} = 7 \text{ TeV}$  is presented. The Higgs boson mass ranges 146 - 230 GeV, 256 - 282 GeV and 296 - 459 GeV are excluded at 95% Confidence Level, while the range 131 - 450 GeV is expected to be excluded in the absence of a signal. Searches in several decay channels are discussed:  $H \rightarrow \gamma\gamma$ ,  $H \rightarrow b\bar{b}$ ,  $H \rightarrow \tau^+\tau^-$ ,  $H \rightarrow ZZ^{(*)} \rightarrow l^+l^-l'^+l'^-$ ,  $H \rightarrow WW^{(*)} \rightarrow l\bar{l}l\bar{l}$ ,  $H \rightarrow WW \rightarrow l\nu qq$ ,  $H \rightarrow ZZ \rightarrow ll\nu\nu$ ,  $H \rightarrow ZZ \rightarrow llqq$ . No significant excess was observed in any of these channels for the entire mass range from 110 to 600 GeV. In addition, a search for neutral Higgs bosons in the Minimal Supersymmetric extension to the Standard Model (MSSM) is presented.

PoS (THEP-LHC-2011) 022

*LHC on the March,  
November 16-18, 2011  
Protvino, Moscow region, Russian Federation*

---

<sup>\*</sup>Speaker.

<sup>†</sup>On behalf of the ATLAS Collaboration

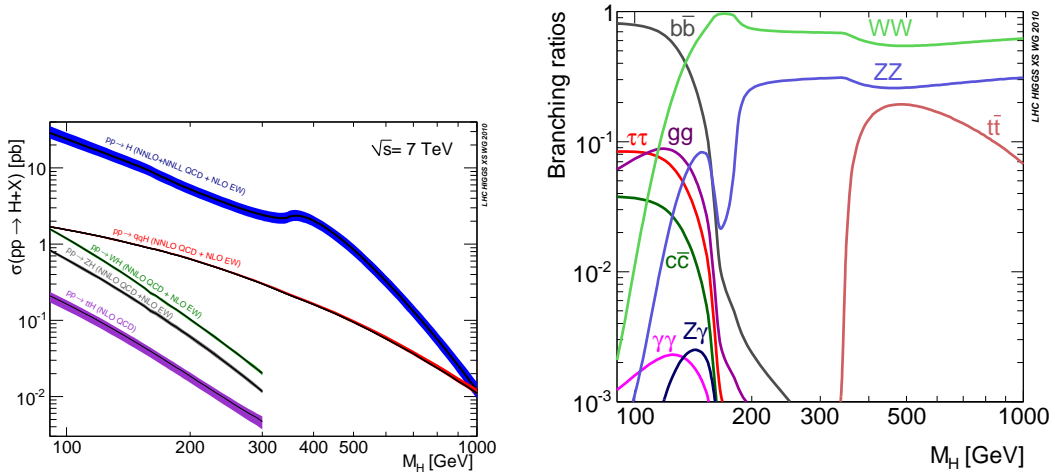


**Figure 1:** (Left) SM Higgs boson production cross section and (right) branching ratios as a function of  $M_H$  at the LHC at  $\sqrt{s} = 7$  TeV [11].

## 1. Introduction

The search for the Standard Model (SM) Higgs boson [1–7] is one of the major goals of the Large Hadron Collider (LHC) at CERN. Direct searches at the CERN LEP  $e^+e^-$  collider excluded a SM Higgs with a mass below 114.4 GeV at 95% Confidence Level (CL) [8]. The searches at the Fermilab Tevatron  $p\bar{p}$  collider have excluded the Higgs boson mass ( $M_H$ ) range between 156 – 177 GeV at 95% CL [9]. Both ATLAS and CMS collaborations have reported very exciting results on Higgs boson searches in 2011 thanks to the outstanding performance of the LHC. In the following, results from the ATLAS experiment corresponding to an analysed integrated luminosity from 1.0 to  $2.3 \text{ fb}^{-1}$  and covering the mass range from 110 to 600 GeV are outlined in Section 3. The combination of the various decay channels is reported in Section 4. Finally, in Section 5, MSSM neutral Higgs bosons searches decaying into a pair of  $\tau$  leptons are reported. Updated results with an integrated luminosity of  $4.9 \text{ fb}^{-1}$  for the ATLAS experiment could be found in [10], but will not be described here.

## 2. Standard Model Higgs boson at the LHC

### 2.1 The Higgs production

At the LHC, the SM Higgs boson can be produced through the following four main mechanisms (see Figure 1): gluon fusion through a heavy quark triangular loop, vector boson fusion (VBF) where vector bosons are radiated from quarks and couple to produce a Higgs boson, associated production with vector bosons W or Z (VH) where the Higgs boson is radiated from a gauge boson, and production in association with a top quark pair ( $t\bar{t}H$ ) where the Higgs boson is radiated from a top quark (for details see [11]). The gluon fusion process has the largest cross section over the whole mass range. The QCD radiative corrections at next-to-next-to-leading order (NNLO) were calculated in the large  $M_H$  limit in addition to the improvement provided by the QCD soft-gluon resummations up to next-to-next-to-leading log (NNLL) together with next-to-leading

order (NLO) electroweak (EW) corrections [12–14]. The remaining theoretical uncertainty is of the order of 15%. The vector boson fusion (VBF) is a very important process since it leaves a special signature in the detector. This process has been computed fully at NLO (EW and QCD corrections). Approximate NNLO QCD corrections have been computed [15], leaving a theoretical uncertainty of the order of 5%. Finally, the Higgs boson VH and  $t\bar{t}H$  associated production modes have been calculated at NNLO [16] and NLO [17–19] respectively.

## 2.2 The Higgs decay modes

In the low mass range ( $100 \leq M_H \lesssim 150$  GeV), the Higgs boson decays into a  $b\bar{b}$  pair with a high branching fraction but the QCD background is expected to be prohibitively large. However the production of the Higgs boson in association with an EW boson is likely to be a more promising process to identify  $H \rightarrow b\bar{b}$  decays due to the reduction in background and the improved trigger signature provided by the leptonic decays of the vector boson. The  $H \rightarrow \tau^+\tau^-$  channel has a smaller branching ratio, about 7%, but offers a signature which can be discriminated from background processes. The sensitivity is enhanced by requiring that the Higgs boson is produced in association with jets, at NLO in the gluon fusion process and at LO in the VBF process. Despite its small branching ratio, about 0.2%, the  $H \rightarrow \gamma\gamma$  is one of the most promising search channels at the LHC because it provides a good experimental sensitivity. The signal would appear as a narrow peak over a continuum of background.

In the high mass range ( $M_H > 150$  GeV), the WW decay mode of the Higgs boson becomes the dominant one. For masses around 160 GeV, the purely leptonic mode  $H \rightarrow WW^{(*)} \rightarrow l\nu\nu$  is the most sensitive channel. For  $M_H > 200$  GeV,  $H \rightarrow WW \rightarrow l\nu qq$  also becomes important, and has an advantage over the  $H \rightarrow WW^{(*)} \rightarrow l\nu\nu$  which is the ability to fully reconstruct the Higgs boson mass. Also a significant fraction of Higgs bosons decay into two Z bosons, for  $M_H > 2M_Z$ . The  $H \rightarrow ZZ^{(*)} \rightarrow l^+l^-l'^+l'^-$  decay mode, where  $l, l' = e, \mu$ , has the cleanest signature for the search for the Higgs boson. In this “golden” channel, an excellent energy and transverse momentum resolution of the reconstructed electrons and muons, respectively, leads to a narrow four-lepton invariant mass peak on top of a smooth background. For  $M_H > 200$  GeV,  $H \rightarrow ZZ \rightarrow llqq$  and  $H \rightarrow ZZ \rightarrow ll\nu\nu$  become also important.

## 3. Standard Model Higgs boson searches

### 3.1 $H \rightarrow \gamma\gamma$

The  $H \rightarrow \gamma\gamma$  analysis is carried out for  $M_H$  hypotheses between 110 and 150 GeV for an integrated luminosity of  $1.08 \text{ fb}^{-1}$  [20]. Two isolated well-identified photons with transverse momenta above 40 and 25 GeV, respectively, are selected. The main background components are the diphoton production, the photon-jet production with one fake photon from jets fragmenting into a leading  $\pi^0$ , the dijet production with two fake photons, and Drell-Yan events where both electrons are misidentified as photons. A data-driven method is used to estimate the fake photon background components from data using control regions for two discriminating variables based on isolation and identification cuts. The Drell-Yan background is estimated by measuring the probability for an electron to be reconstructed as a photon candidate with Z events and applying it to the observed

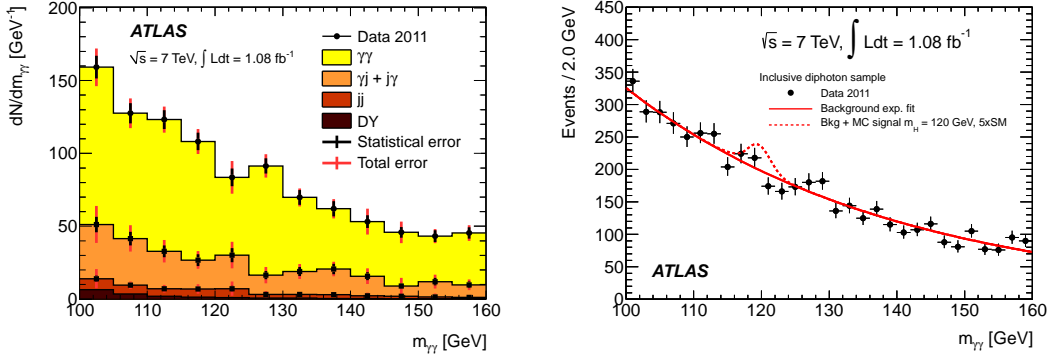


**Figure 2:** Left: Decomposition of the diphoton candidate invariant mass distribution, as obtained from a data-driven method. The components are stacked on top of each other. Right: Invariant mass distribution from the selected data sample for all categories together. The exponential fit to the full sample of the background-only hypothesis, as well as the expected signal for a Higgs boson mass of 120 GeV with five times the SM predicted yield, are also shown for illustration [20].

yield of Drell-Yan events at high mass. Figure 2 (left) shows the extracted background components from data. The purity of the sample (fraction of diphoton events) is about 72%.

The analysis in this channel splits the selected events into five categories with different invariant mass resolutions and signal-to-background ratios in order to enhance the sensitivity. The categorization is based on the direction in which each photon was emitted and whether or not it is reconstructed as a converted photon. The vertex position is estimated from the shower position in the the first and second layers of the calorimeter for unconverted photons, while for converted photons it is estimated from the intercept of the line joining the reconstructed conversion position and the calorimeter impact point with the beam line. When both photons are unconverted, the vertex position resolution is about 1.6 cm in z and it is even better in case of converted photons.

The mass resolution for the signal is modelled by the sum of a Crystal-Ball function and a Gaussian distribution with a wide sigma. The background is estimated from an unbinned fit of the di-photon mass spectrum with a single exponential. Figure 2 (right) shows the reconstructed diphoton mass spectrum; no significant excess is visible. Experimental systematic uncertainties were estimated to be about  $\pm 12\%$  on the expected signal yield and  $\pm 14\%$  on the di-photon invariant mass resolution. An additional systematic uncertainty is computed to take into account possible deviations of the background distribution from the exponential shape. All the systematic uncertainties are treated as fully correlated between the various categories. The test statistic used is a profile likelihood ratio and the method used (as well as for the other channels) to set exclusion limits is the modified-frequentist approach  $CL_s$  [21]. The expected median limit varies from 3.3 to 5.8 times the SM cross section as a function of the Higgs mass. The observed limit varies between 2.0 and 5.8 times the SM cross section within the expected statistical fluctuations around the median limit.

### 3.2 $H \rightarrow b\bar{b}$ : $W/H(l\nu b\bar{b})$ and $Z/H(l l b\bar{b})$

The search for the SM Higgs boson produced in association with a  $W$  or  $Z$  boson decaying to  $b\bar{b}$  is performed in the mass range between 110 and 130 GeV for an integrated luminosity of  $1.04 \text{ fb}^{-1}$  [22].

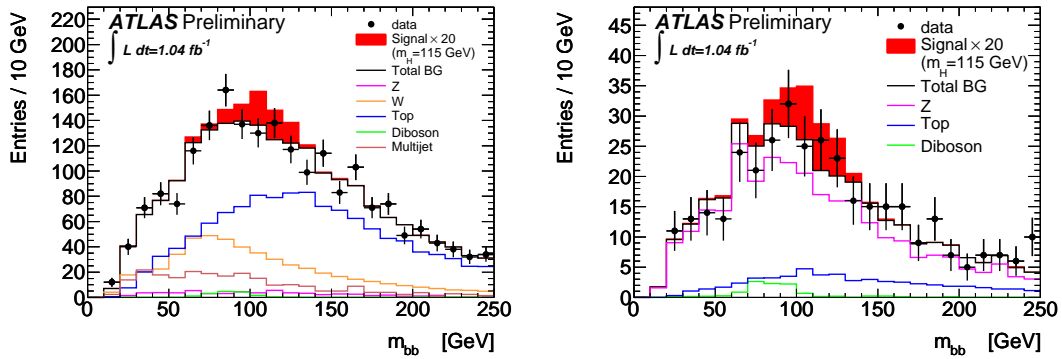


**Figure 3:** The invariant mass,  $m_{bb\bar{b}}$ , for  $WH \rightarrow lbb\bar{b}$  (left) and  $ZH \rightarrow ll\bar{b}\bar{b}$  (right) for  $M_H = 115$  GeV. The signal distribution is enhanced by a factor 20 for visibility [22].

In the  $ZH \rightarrow ll\bar{b}\bar{b}$  search channel, the selection requires a reconstructed  $Z$  candidate and a small  $E_T^{miss}$ . The invariant mass of the two leptons is required to lie within 15 GeV from the  $Z$  mass to suppress background coming from  $t\bar{t}$  and multijet production. In addition, at least two b-tagged jets with  $p_T > 25$  GeV are required. The dominant background to the  $Z/H(ll\bar{b}\bar{b})$  is expected to come from  $Z+jets$  events. It is estimated using a data control region for normalisation and simulation for a shape template. Other backgrounds from  $t\bar{t}$  production, multijet and  $ZZ/WZ$  production also contribute and are estimated from simulation. The background coming from top production was also checked in the sidebands of the di-lepton invariant mass distribution.

In the  $WH \rightarrow lbb\bar{b}$  channel, events are characterized by exactly one lepton originating from  $W$  decay and significant  $E_T^{miss}$ . Exactly two jets with  $p_T > 25$  GeV are required to reduce background from top quark production  $t\bar{t} \rightarrow bW(l\nu)\bar{t}W(q\bar{q})$ . These jets have to be b-tagged to reduce background from  $W+jets$ . The dominant backgrounds arise from top-quark production, QCD multijet production and  $W+jets$ . These backgrounds are determined by a simultaneous template fit to data control regions. The top and  $W+jets$  templates are determined from Monte-Carlo simulation for  $t\bar{t}$  events and un-tagged  $W+jets$  events from data.

The di-b-jet invariant mass  $m_{bb\bar{b}}$  distributions for  $ZH \rightarrow ll\bar{b}\bar{b}$  and  $WH \rightarrow lbb\bar{b}$  for  $M_H = 115$  GeV are shown in Figure 3. The resulting exclusion limits range between 10 to 20 times the SM cross section, when combining both channels, depending on the Higgs mass.

### 3.3 $H \rightarrow \tau^+\tau^-$

This search is performed as a counting analysis for Higgs boson mass hypotheses between 110 GeV and 150 GeV, in the  $H \rightarrow \tau\tau \rightarrow l^+l^- + 4\nu$  [23] and  $H \rightarrow \tau\tau \rightarrow l\tau_{had}3\nu$  [24] channels, for an integrated luminosity of  $1.06 \text{ fb}^{-1}$ .

In the fully-leptonic  $\tau$ -final state, the selection requests two high- $p_T$  leptons and at least one jet with  $p_T > 40$  GeV. The resulting boost of the Higgs boson implies a large  $E_T^{miss}$  in the event. The large  $E_T^{miss}$  and the high- $p_T$  jet allow for a good discrimination against background processes such as  $Z/\gamma^* \rightarrow ll$ ,  $Z \rightarrow \tau^+\tau^-$  and QCD multi-jet events. The  $Z \rightarrow ll$  background is further reduced when the two leptons are from the same flavour by requiring that the mass of the dilepton is substantially smaller than the mass of the  $Z$  boson.  $Z \rightarrow \tau^+\tau^-$  is the main background in this analysis, its

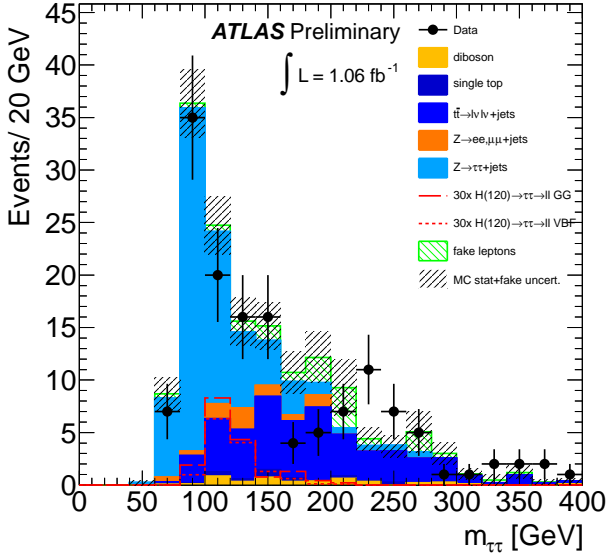


**Figure 4:**  $m_{\tau\tau}$  invariant mass after the analysis cuts for  $ee, \mu\mu$  and  $e\mu$  channels. The backgrounds with fake leptons and the  $Z \rightarrow \tau^+\tau^-$  contribution are estimated from data. All other contributions are estimated using simulated event samples [23].

invariant mass shape is estimated using an embedding technique where muons from  $Z \rightarrow \mu\mu$  events are replaced by simulated  $\tau$  decays. The top-quark pair production, single top,  $Z \rightarrow ll$  and EW diboson production backgrounds are estimated from simulation. The QCD background is estimated within an independent control sample. The remaining challenge is to reconstruct the invariant mass of the  $\tau$ -lepton system ( $m_{\tau\tau}$ ). This is done using the collinear approximation [25], where the neutrinos are produced from the  $\tau$  decay along the direction of the visible leptons. The obtained  $m_{\tau\tau}$  distribution is shown in Figure 4.

In the semi-leptonic  $\tau$  - final state,  $H \rightarrow \tau\tau \rightarrow l\tau_{had}3\nu$ , the selection requires one high- $p_T$  lepton and an oppositely charged tau candidate ( $\tau_{had}$ ) with  $p_T > 20$  GeV. Events with an additional lepton are removed to suppress the  $Z/\gamma^* \rightarrow ll$  and  $t\bar{t}$ . The  $W \rightarrow l\nu$  background is suppressed by requiring the transverse mass of the lepton and missing energy system to be smaller than 30 GeV. To compute the invariant mass of the pair of tau leptons, a new mass reconstruction technique is used, the so-called missing mass calculator (MMC) technique, which does not assume a strict collinearity between the visible and invisible decay products of the tau leptons [26]. The  $H \rightarrow \tau\tau \rightarrow l\tau_{had}3\nu$  channel is significantly more sensitive than the  $H \rightarrow l^+l^- + 4\nu$  channel. The combined exclusion limit for both channels at 95% CL is around 10 times the SM cross section.

### 3.4 $H \rightarrow ZZ^{(*)} \rightarrow 4l$

The search for the Higgs boson in the  $H \rightarrow ZZ^{(*)} \rightarrow 4l$  decay channel is performed for mass hypotheses between 110 and 600 GeV for an integrated luminosity of 2.0-2.3  $\text{fb}^{-1}$  [27]. Three distinct final states,  $4e$ ,  $2e2\mu$ ,  $4\mu$ , are selected. The selection requires two same-flavour, opposite-sign isolated lepton pairs, with one di-lepton mass compatible with the  $Z$  boson mass ( $m_{12}$ ) within

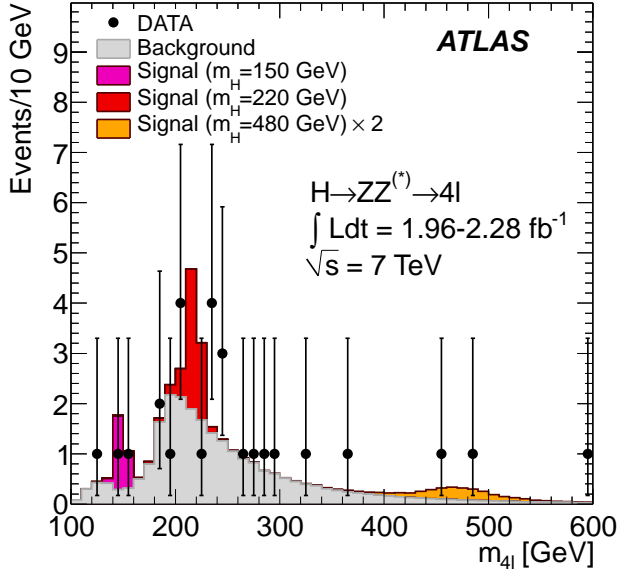


**Figure 5:** The  $m_{4l}$  distribution; the signal expectations for three  $M_H$  hypotheses are also shown as well as the total background prediction [27].

15 GeV and the second di-lepton mass ( $m_{34}$ ) lower than 115 GeV and greater than a threshold depending on the reconstructed four lepton mass ( $m_{4l}$ ). The main background is the  $ZZ^{(*)}$  continuum, which is estimated from simulation. The reducible  $Z+jets$  background is estimated from data control regions, while the  $t\bar{t}$  background is estimated from simulation. The width of the reconstructed Higgs boson mass distribution is dominated by experimental resolution at low mass values, with a full-width at half-maximum (FWHM) which varies according to decay mode and is between 4.5 (4 $\mu$ ) and 6.5 (4e) GeV for  $M_H = 130$  GeV. At high mass, the reconstructed width is dominated by the natural width of the Higgs boson with a FWHM of approximately 35 GeV at  $M_H = 400$  GeV. Twenty-seven candidates were observed. The  $m_{4l}$  distribution for the total background and several signal hypotheses is compared to data in Figure 5. All detector and luminosity-related systematic uncertainties are taken to be fully correlated between signal and background. The most significant deviation observed from the background-only hypothesis occurs at  $M_H = 242$  GeV with a p-value of 4.9%. These results do not take into account the so-called look-elsewhere effect [28]. The SM Higgs boson is excluded at 95% CL in the mass ranges 191 – 197, 199 – 200 and 214 – 224 GeV.

### 3.5 $H \rightarrow WW^{(*)} \rightarrow l\nu l\nu$

This search is performed as a counting analysis for Higgs boson mass hypotheses between 110 GeV and 300 GeV for an integrated luminosity of  $1.70 \text{ fb}^{-1}$  [29]. After selection of exactly two isolated oppositely charged leptons, the significant backgrounds are the production of  $Z/\gamma^*+jets$ ,  $t\bar{t}$  and single top,  $WW$ ,  $WZ$ ,  $ZZ$ ,  $W\gamma$  and  $W+jets$  where a jet is misidentified as a lepton. The background from  $W+jets$  is entirely estimated from data using a control sample where one of the two leptons satisfies a loosened set of identification and isolation criteria. The other background

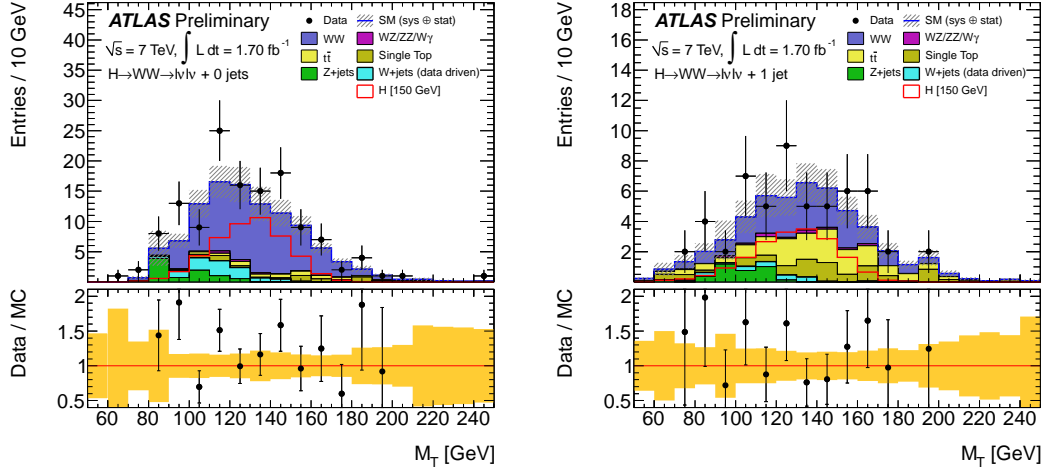


**Figure 6:** The transverse mass  $m_T$  distribution in the H+0 (left) and H+1 (right) jet analysis after all the cuts except the cut on  $m_T$  itself. The expected signal is shown for  $M_H = 150$  GeV. The lower part of the plot shows the ratio between the data and the background expectation from MC, with the yellow band indicating the total systematic uncertainty in the normalization (but not the shape) of the various components. The final bin includes the overflow [29].

processes are determined from simulation, with  $Z/\gamma^*+$ jets,  $WW$ ,  $t\bar{t}$  and single top corrected by scale factors derived from control samples.

The dilepton invariant mass ( $m_{ll}$ ) is required to be above 10 GeV if the two leptons are of different flavour. Otherwise  $m_{ll}$  is required to satisfy  $m_{ll} > 15$  GeV and  $|m_{ll} - m_Z| > 15$  GeV to suppress backgrounds from  $\Upsilon$  and  $Z$  production respectively. The remaining QCD and Drell-Yan events are suppressed by a requirement on the missing transverse energy  $E_{T,\text{rel}}^{\text{miss}}$ . The quantity  $E_{T,\text{rel}}^{\text{miss}}$  is defined as  $E_T^{\text{miss}}$  if the angle  $\Delta\phi$  between the missing transverse momentum and the nearest lepton or jet in the transverse plane is  $\Delta\phi > \pi/2$  or  $E_T^{\text{miss}} \sin(\Delta\phi)$  otherwise.  $E_{T,\text{rel}}^{\text{miss}}$  is required to be above 40 GeV if the two leptons have the same flavour and above 25 GeV otherwise. The analysis is then separated into two categories: H + 0-jet and H + 1-jet. The dilepton system in the H + 0-jet category is required to have a large transverse momentum  $p_T^{ll} > 30$  GeV to further suppress backgrounds from  $Z+$ jets and  $WW$ . In the H + 1-jet category, events are rejected if the jet is tagged as originating from a  $b$ -quark to suppress the background from top-quark production. An upper bound on  $m_{ll}$  is applied depending on  $M_H$  to suppress backgrounds from top and  $WW$  production. For  $M_H < 220$  GeV, an upper bound is imposed on the azimuthal angle between the two leptons:  $\Delta\phi_{ll} < 1.3$  (1.8) radians for  $M_H < 170$  GeV ( $M_H \geq 170$  GeV). Finally, the transverse mass is required to satisfy  $0.75 \times M_H < m_T < M_H$  if  $M_H < 220$  GeV and  $0.6 \times M_H < m_T < M_H$  otherwise. The transverse mass distributions (before the last cut) of the candidates in the H + 0-jet and H + 1-jet categories are shown in Figure 6.

No significant excess is observed. A SM Higgs boson is excluded at 95% CL from 154 to 186 GeV.

### 3.6 $H \rightarrow WW \rightarrow llqq$

The search of the SM Higgs boson when decaying to  $WW \rightarrow llqq$  is performed in the mass range between 240 GeV to 600 GeV for an integrated luminosity of  $1.04 \text{ fb}^{-1}$  [30]. The selection

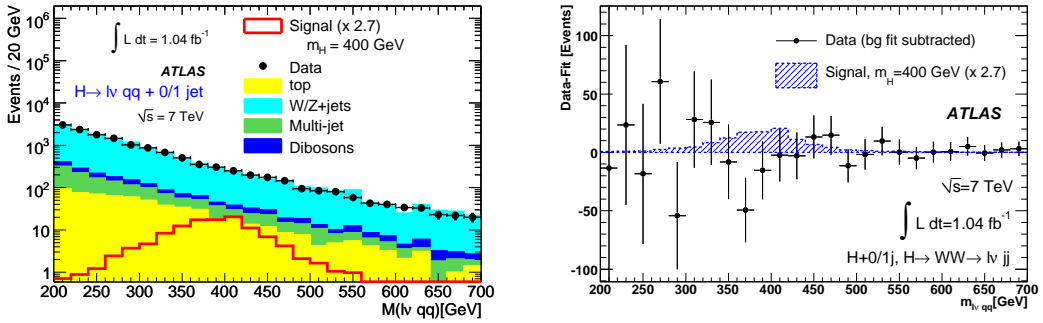


**Figure 7:** Left: the reconstructed invariant mass  $m_{lvqq}$  in the data summed over lepton flavour and jet multiplicity. The expected backgrounds are also shown. Right: the difference between data and the fitted non-resonant background. The expected contribution from Higgs boson decays for  $M_H = 400$  GeV in the SM is also shown, multiplied by a factor of 2.7 [30].

requires exactly one lepton with  $p_T > 30$  GeV and a missing transverse energy above 30 GeV. The analysis is separated into two samples H + 0-jet and H + 1-jet. A  $b$ -jet veto is applied in the H + 1-jet category to reduce background from top production. After this selection, the background is dominated by  $W$ +jets production. Other important background processes are  $Z$ +jets, QCD multijet, top quark and diboson ( $WW$ ,  $WZ$ ,  $ZZ$ ) production. The background modeling is estimated from simulation for all processes except the QCD multijet where control samples from data are used with loosened identification and isolation set criteria.

In order to reconstruct the invariant mass  $m_{lvqq}$ , a mass constraint  $m_{lv} = m_W$  is applied. The  $m_{lvqq}$  distribution of the selected candidates is illustrated in Figure 7 (left) where an expected signal, scaled by a factor of 2.7, at  $M_H = 400$  GeV is also shown. A fit to data with a double exponential is used as to model the background. In Figure 7 (right) the difference between the  $m_{lvqq}$  distribution in data and the fitted background is shown. No significant excess is observed and an upper limit of 2.7 times the SM cross section is set for a Higgs boson mass of 400 GeV.

### 3.7 $H \rightarrow ZZ \rightarrow llvv$

The search in this channel is carried out for the 200 to 600 GeV mass range of the Higgs boson hypothesis using a data sample corresponding to an integrated luminosity of  $2.05 \text{ fb}^{-1}$  [31]. The analysis is divided into a high ( $> 280$  GeV) and a low mass region. Events are required to contain exactly two oppositely charged leptons where the dilepton invariant mass must satisfy  $|m_{ll} - m_Z| < 15$  GeV in order to suppress backgrounds from top quark,  $W$  boson and QCD multijet production. In addition, events with an azimuthal angle between the missing transverse momentum and the leading jet in the event  $\Delta\phi < 0.3$  are rejected to reduce background from events with fake  $E_T^{\text{miss}}$  due to mismeasured jets. To reduce background from top quark production, events with one or more  $b$ -tagged jets are also rejected. The main background at high transverse mass values is the di-boson production  $ZZ$ ,  $WW$  and  $WZ$ , which are estimated from simulation. The  $Z$ +jets and top production are estimated from MC, the  $W$ +jets and QCD multijet production are estimated from data. The results obtained show no evidence for a signal and an exclusion at 95% CL of the SM Higgs cross section is obtained in the mass range from 310 to 470 GeV.

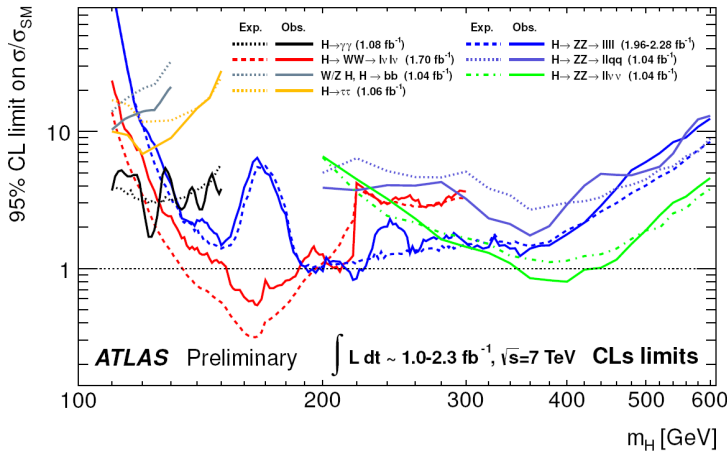


**Figure 8:** The expected (dashed) and observed (solid) cross section limits for the individual search channels, normalised to the Standard Model Higgs boson cross section, as functions of the Higgs boson mass. These results use the profile likelihood ratio technique with 95% CL limits using the  $CL_s$  construction [24].

### 3.8 $H \rightarrow ZZ \rightarrow llqq$

The analysis in the  $H \rightarrow ZZ \rightarrow llqq$  channel is performed in the mass range from 200 GeV to 600 GeV for an integrated luminosity of  $2.05 \text{ fb}^{-1}$  [32] and it is separated into two regions: below and above 300 GeV. Events are selected by requiring a pair of leptons with  $|m_{ll} - m_Z| < 15 \text{ GeV}$  and a pair of high- $p_T$  jets with their invariant mass constrained to the mass of the Z boson. The missing transverse energy has to be below 50 GeV. The selected events are further divided into two categories: events with two  $b$ -tagged jets (i.e.  $H \rightarrow ZZ \rightarrow llb\bar{b}$ ) and the rest. The small number of events with more than two  $b$ -tagged jets are rejected. The dominant Z+jets background is normalized from a control region defined by the sidebands of the di-jet mass distribution. The less important contribution from top quark production is estimated from simulation. In order to suppress the Z+jets background for a Higgs mass above 300 GeV, additional cuts are applied: The azimuthal angle between the two leptons and the two jets must satisfy respectively  $\Delta\phi_{ll} < 90^\circ$  and  $\Delta\phi_{jj} < 90^\circ$  and the two jets must have  $p_T > 45 \text{ GeV}$ . The final discriminant in this analysis is the di-lepton di-jet invariant mass, the shape of which is estimated from MC for both signal and background processes. No significant excesses are seen in the resulting invariant mass distributions. Observed upper limits, at 95% CL, of between 1.2 and 12 times the SM cross section, depending on the Higgs boson mass, are obtained.

## 4. Combined Results

All the channels described above, except  $H \rightarrow WW \rightarrow llqq$ , were combined in ATLAS [24] following the procedure described in Refs. [34, 33, 35]. The 95% CL exclusion limits in units of a SM cross section for the different individual channels are shown in Figure 8. The limits shown are computed using the asymptotic approximation [36], their agreement with MC pseudo-experiments and with the Bayesian approach was verified to be within a few percent [34]. The expected 95%

CL combined exclusion covers the SM Higgs boson mass range from 131 GeV to 450 GeV. The observed 95% CL combined exclusion ranges from 146 GeV to 230 GeV, 256 GeV to 282 GeV and 296 GeV to 459 GeV. The exclusion CL is about 99% in the region between 160 GeV and 220 GeV and exceeds 99% between 300 GeV and 420 GeV. The highest significance is about  $2\sigma$  for an excess around 144 GeV, thus consistent with an upward fluctuation of the background.

## 5. MSSM Higgs Searches

### 5.1 $A/H/h \rightarrow \tau^+\tau^-$

The search for neutral MSSM Higgs bosons decaying into a pair of  $\tau$ -leptons was performed using an integrated luminosity of  $1.06 \text{ fb}^{-1}$  [37] in the four final states:  $\tau\tau \rightarrow e\mu 4\nu$ ,  $e\tau_{had}3\nu$ ,  $\mu\tau_{had}3\nu$  and  $\tau_{had}\tau_{had}2\nu$ .

In the  $e\mu 4\nu$  final state, the selection requires one isolated electron, one isolated muon and a missing transverse energy. The  $t\bar{t}$ , single-top and di-boson backgrounds are suppressed with two additional requirements: the scalar sum of the transverse momentum of the electron, the transverse momentum of the muon and the missing transverse momentum must be smaller than 120 GeV, and the azimuthal opening angle between the electron and the muon must be larger than 2.0 rad. An effective mass reconstruction  $m_{\tau\tau}^{eff}$ , i.e calculating the invariant mass of the visible tau decay products and the  $E_T^{miss}$  system, is used in this final state.

In the  $e/\mu\tau_{had}3\nu$  final state, one decaying leptonically  $\tau$  lepton and an other hadronically with a missing transverse energy are required. Events with more than one reconstructed lepton, using loose lepton identification cuts, are rejected to suppress background from  $Z/\gamma^* \rightarrow l^+l^-$  and from  $t\bar{t}$  or single-top production. The missing transverse energy is required to be above 20 GeV to suppress events with jets from QCD processes and the transverse mass of the  $l-E_T^{miss}$  system is required to be below 30 GeV to suppress events with real leptons from  $W \rightarrow l\nu$  decays. The invariant mass  $m_{\tau\tau}$  is reconstructed using the MMC technique.

Finally, in the  $\tau_{had}\tau_{had}2\nu$  final state, the selection requires exactly two oppositely charged  $\tau_{had}$  candidates with  $p_T > 45(30)$  GeV and a missing transverse energy  $E_T^{miss} > 25$  GeV to suppress background from  $Z$ ,  $W$  boson and QCD multijet production. Events are rejected if they contain an electron with  $p_T^e > 15$  GeV or a muon candidate with  $p_T^\mu > 10$  GeV; isolation is not required. The invariant mass  $m_{\tau\tau}^{vis}$  is computing using the visible tau decay products.

No significant excess of events is found. Exclusion limits at the 95% CL are set on the production cross section times branching ratio,  $\sigma \times BR(\phi \rightarrow \tau^+\tau^-)$ , of a generic Higgs boson  $\phi$  as a function of its mass,  $m_\phi$ , and for MSSM Higgs boson  $A/H/h$  production as a function of the parameters  $m_A$  and  $\tan\beta$  (see Figure 9 (right)). The  $l\tau_{had}$  final state provides the most stringent limit. The  $e\mu$  and  $\tau_{had}\tau_{had}$  channels lead to improvements of the exclusion limits for small and high Higgs boson masses respectively.

## 6. Conclusions

With  $1.04\text{-}2.28 \text{ fb}^{-1}$  of analysed data, no significant evidence of a SM Higgs boson production is observed in the ATLAS experiment. The SM Higgs boson is excluded at 95% CL in the mass ranges from 146 to 230 GeV, 256 to 282 GeV and 296 to 459 GeV. The confidence level reaches

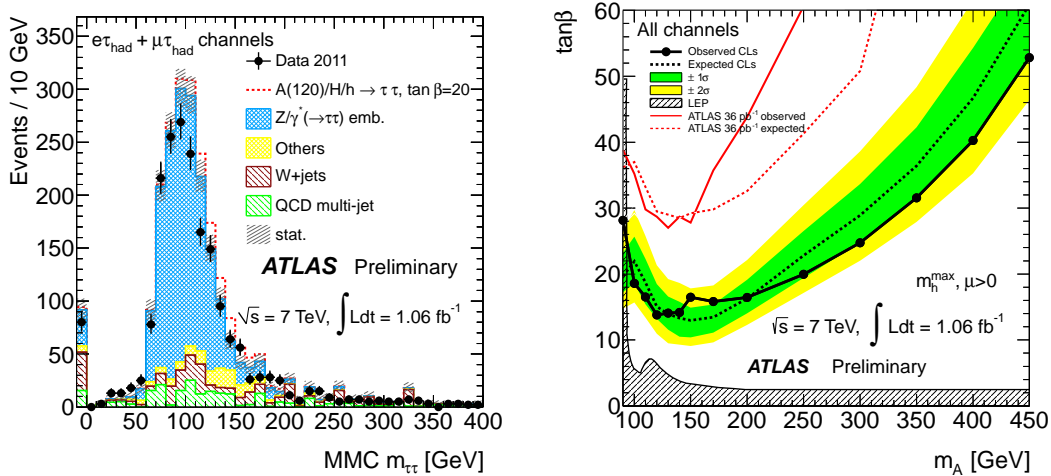


**Figure 9:** Left: shows the di-tau mass distribution computed with the MMC technique [26] for  $e\tau_{had}$  and  $e\tau_{had}$  final state channels. Right: expected and observed exclusion limits based on  $CL_s$  in the  $m_A - \tan\beta$  plane of the MSSM derived from the combination of the analyses for the  $e\mu, l\tau_{had}$  and  $\tau_{had}\tau_{had}$  final states. The exclusion limits from a previous result and from LEP are also shown [37].

99% for the region between 160 and 220 GeV and exceeds 99% between 300 and 420 GeV. When combining these results with recent results from CMS [38], for an integrated luminosity going from 1.0 to 2.3  $\text{fb}^{-1}$  depending on the channel, the SM Higgs boson is excluded at 95% CL from 141 to 476 GeV and at 99% CL from 146 to 443 GeV except for three small mass regions. The most favored remaining search region is at low masses, in the approximate range 114–141 GeV. In addition, exclusion limits on both the cross section for the production of a generic Higgs boson  $\phi$  as a function of its mass and on MSSM Higgs boson production  $A/H/h$  as a function of  $m_A$  and  $\tan\beta$ , are derived. These results exclude regions of parameters space beyond the existing limits from previous experiments at LEP [39] and the Tevatron [40, 41].

## References

- [1] P. Anderson, *Plasmons, Gauge Invariance, and Mass*, Phys. Rev. **130**, 439 (1963).
- [2] F. Englert and R. Brout, *Broken Symmetry and the Mass of Gauge Vector Mesons*, Phys. Rev. Lett. **13**, 321 (1964).
- [3] P. Higgs, *Broken Symmetries, massless particles and gauge fields*, Phys. Lett. **12**, 132 (1964).
- [4] P. Higgs, *Broken Symmetries and the Masses of Gauge Bosons*, Phys. Rev. Lett. **13**, 508 (1964).
- [5] G. S. Guralnik, C. R. Hagen and T. W. B. Kibble, *Global Conservation Laws and Massless Particles*, Phys. Rev. Lett. **13**, 585 (1964).
- [6] P. Higgs, *Spontaneous Symmetry Breakdown without Massless Bosons*, Phys. Rev. **145**, 1156 (1966).
- [7] T. Kibble, *Symmetry breaking in nonAbelian gauge theories*, Phys. Rev. **155**, 1554 (1967).
- [8] LEP Working Group for Higgs boson searches (R. Barate *et al.*), *Search for the Standard Model Higgs boson at LEP*, Phys. Lett. B **565**, 61 (2003).

- [9] The TEVNPH Working Group of the CDF and DØ Collab., *Combined CDF and DØ upper limits on Standard Model Higgs-boson production with up to  $8.6 \text{ fb}^{-1}$  of data*, arXiv:1107.5518 [hep-ex].
- [10] ATLAS Collab., *Combined Search for the Standard Model Higgs boson using up to  $4.9 \text{ fb}^{-1}$  of pp collision data of  $\sqrt{s} = 7 \text{ TeV}$  with the ATLAS detector at the LHC*, CERN-PH-EP-2012-019, CERN, Geneva, 2011; arXiv:1202.1408 [hep-ph].
- [11] LHC Higgs Cross Section Working Group (S. Dittmaier, C. Mariotti, G. Passarino, and R. Tanaka (Eds.)), *Handbook of LHC Higgs Cross Sections: 1. Inclusive Observables*, CERN-PH-EP-2011-002, CERN, Geneva, 2011; arXiv:1101.0593 [hep-ph].
- [12] Charalampos Anastasiou and Kirill Melnikov, *Higgs boson production at hadron colliders in NNLO QCD*, Nucl. Phys. B **646**, 220 (2002).
- [13] Robert V. Harlander and William B. Kilgore, *Next-to-next-to-leading order Higgs production at hadron colliders*, Phys. Rev. Lett. **88**, 201801 (2002).
- [14] V. Ravindran, J. Smith, and W. L. van Neerven, *NNLO corrections to the total cross section for Higgs boson production in hadron hadron collisions*, Nucl. Phys. B **665**, 325 (2003).
- [15] Paolo Bolzoni, Fabio Maltoni, Sven-Olaf Moch and Marco Zaro, *Higgs production via vector-boson fusion at NNLO in QCD*, Phys. Rev. Lett. **105**, 011801 (2010).
- [16] O. Brein, A. Djouadi and R. Harlander, *NNLO QCD corrections to the Higgsstrahlung processes at hadron colliders*, Phys. Lett. B **579**, 149 (2004).
- [17] W. Beenakker *et al.*, *Higgs radiation off top quarks at the Tevatron and the LHC*, Phys. Rev. Lett. **87**, 201805 (2001).
- [18] W. Beenakker *et al.*, *NLO QCD corrections to  $t$  anti- $t$  H production in hadron collisions*, Nucl. Phys. B **653**, 151 (2003).
- [19] S. Dawson, L. H. Orr, L. Reina and D. Wackeroth, *Associated top quark Higgs boson production at the LHC*, Phys. Rev. D **67**, 071503 (2003).
- [20] ATLAS Collab., *Search for the Standard Model Higgs boson in the two photon decay channel with the ATLAS detector at the LHC*, CERN-PH-EP-2011-129, CERN, Geneva, 2011; arXiv:1108.5895 [hep-ph]; Phys. Lett. B **705**, 452 (2011).
- [21] A. Read, *Presentation of search results: the  $CL_s$  technique*, J. Phys. G **28**, 2693 (2002).
- [22] ATLAS Collab., *Search for the Standard Model Higgs boson produced in association with a vector boson and decaying to a b-quark pair with the ATLAS detector at the LHC*, ATLAS-CONF-2011-103, CERN, Geneva, 2011.
- [23] ATLAS Collab., *Search for the Standard Model Higgs boson in the Decay Mode  $H \rightarrow \tau^+ \tau^- \rightarrow ll + 4$  Neutrinos in Association with Jets in Proton-Proton Collisions at  $\sqrt{s} = 7 \text{ TeV}$  with the ATLAS Detector*, ATLAS-CONF-2011-133, CERN, Geneva, 2011.
- [24] ATLAS Collab., *Update of the Combination of Higgs Boson Searches in 1.0 to  $2.3 \text{ fb}^{-1}$  of pp Collisions Data Taken at  $\sqrt{s} = 7 \text{ TeV}$  with the ATLAS Experiment at the LHC*, ATLAS-CONF-2011-135, CERN, Geneva, 2011.
- [25] R. K. Ellis, I. Hinchliffe, M. Soldate and J. J. Van der Bij, *Higgs decay to  $\tau^+ \tau^-$ : A possible signature of intermediate mass Higgs bosons at high energy hadron colliders*, Nucl. Phys. B **297**, 221 (1988).
- [26] A. Elagin, P. Murat, A. Pranko and A. Safonov, *A new Mass Reconstruction Technique for Resonances Decaying to di-tau*, arXiv:1012.4686 [hep-ex]; Nucl. Instrum. Meth. A **654**, 481 (2011).

- [27] ATLAS Collab., *Search for the Standard Model Higgs boson in the decay channel  $H \rightarrow 4l$  with the ATLAS detector*, CERN-PH-EP-2011-144, CERN, Geneva, 2011; arXiv:1109.5945 [hep-ph]; Phys. Lett. B **705**, 435 (2011).
- [28] E. Gross and O. Vitells, *Trial factors for the look elsewhere effect in high energy physics*, Particles and Fields Eur. Phys. J. C **70**, 525 (2010).
- [29] ATLAS Collab., *Search for the Standard Model Higgs boson in the  $H \rightarrow WW^{(*)} \rightarrow llvv$  decay mode using  $1.7\text{ fb}^{-1}$  of data collected with the ATLAS detector at  $\sqrt{s} = 7\text{ TeV}$* , ATLAS-CONF-2011-134, CERN, Geneva, 2011.
- [30] ATLAS Collab., *Search for the Higgs boson in the  $H \rightarrow WW \rightarrow lvjj$  decay channel in pp collisions at  $\sqrt{s} = 7\text{ TeV}$  with the ATLAS detector*, CERN-PH-EP-2011-130, CERN, Geneva, 2011; arXiv:1109.3615 [hep-ph]; Phys. Rev. Lett. **107**, 231801 (2011).
- [31] ATLAS Collab., *Search for a Standard Model Higgs boson in the  $H \rightarrow ZZ \rightarrow l^+l^-v\bar{v}$  decay channel with  $2.05\text{ fb}^{-1}$  of ATLAS data*, ATLAS-CONF-2011-148, CERN, Geneva, 2011.
- [32] ATLAS Collab., *Search for a heavy Standard Model Higgs boson in the mass range 200-600 GeV in the channel  $H \rightarrow ZZ \rightarrow l^+l^-q\bar{q}$  using the ATLAS detector*, ATLAS-CONF-2011-150, CERN, Geneva, 2011.
- [33] ATLAS Collab., *Limits on the production of the Standard Model Higgs Boson in pp collisions at  $\sqrt{s} = 7\text{ TeV}$  with the ATLAS detector*, arXiv:1106.2748 [hep-ex]; Eur. Phys. J. C **71**, 1728 (2011).
- [34] ATLAS Collab., *Combination of the Searches for the Higgs Boson in  $\sim 1\text{ fb}^{-1}$  of Data Taken with the ATLAS Detector at 7 TeV Center-of-Mass Energy*, ATLAS-CONF-2011-112, CERN, Geneva, 2011.
- [35] ATLAS and CMS Collaborations, *LHC Higgs Combination Working Group Report*, ATL-PHYS-PUB-2011-818, CERN, Geneva, 2011.
- [36] G. Cowan, K. Cranmer, E. Gross and O. Vitells, *Asymptotic formulae for likelihood-based tests of new physics*, Eur. Phys. J. C **71**, 1 (2011).
- [37] ATLAS Collab., *Search for neutral MSSM Higgs bosons decaying to  $\tau^+\tau^-$  pairs in proton-proton collisions at  $\sqrt{s} = 7\text{ TeV}$  with the ATLAS detector*, ATLAS-CONF-2011-132, CERN, Geneva, 2011.
- [38] ATLAS and CMS Collaborations, *Combined Standard Model Higgs boson searches with up to  $2.3\text{ fb}^{-1}$  of pp collision data at  $\sqrt{s} = 7\text{ TeV}$  at the LHC*, ATLAS-CONF-2011-157, CERN, Geneva, 2011; CMS PAS HIG-11-023, CERN, Geneva, 2011.
- [39] ALEPH Collab., DELPHI Collab., L3 Collab., OPAL Collab. and LEP Working Group for Higgs Boson Searches, *Search for neutral MSSM Higgs bosons at LEP*, Eur. Phys. J. C **47**, 547-587 (2006).
- [40] The CDF and DØ Collaborations and Tevatron New Physics Higgs Working Group (TEVNPHWG), *Combined CDF and DØ upper limits on MSSM Higgs boson production in  $\tau\tau$  final states with up to  $2.2\text{ fb}^{-1}$* , arXiv:1003.3363 [hep-ex].
- [41] The DØ Collab. (V. M. Abazov *et al.*), *Search for neutral Higgs bosons decaying to tau pairs produced in association with b quarks in  $p\bar{p}$  collisions at  $\sqrt{s} = 1.96\text{ TeV}$* , arXiv:1106.4885 [hep-ex], Phys. Rev. Lett. **107**, 121801 (2011).